Biosensors and Bioelectronics 167 (2020) 112512

Contents lists available at ScienceDirect

Biosensors and Bioelectronics

journal homepage: http://www.elsevier.com/locate/bios

Simultaneous cortisol/insulin microchip detection using dual enzyme tagging

Eva Vargas [a], Eloy Povedano [a,b], Sadagopan Krishnan [a,c], Hazhir Teymourian [a], Farshad Tehrani [a], Susana Campuzano [b], Eyal Dassau [d,**], Joseph Wang [a,*]

[a] Department of Nanoengineering, University of California, San Diego, La Jolla, CA, 92093, USA
[b] Departamento de Química Analítica, Universidad Complutense de Madrid, E-28040, Madrid, Spain
[c] Department of Chemistry, Oklahoma State University, Stillwater, OK, 74078, USA
[d] Harvard John A. Paulson School of Engineering and Applied Sciences, Harvard University, Cambridge, MA, 02138, USA

ARTICLE INFO

Keywords:
Biosensors
Immunoassay
Multiplexed detection
Diabetes management
Cortisol sensor
Insulin sensor

ABSTRACT

Here we describe the development of a dual electrochemical immunosensor microchip for simultaneous detection of insulin (I) and cortisol (C) biomarkers that can enhance the ability to improve glucose regulation using automated insulin delivery. The successful realization of the simultaneous I and C measurements has been realized by integrating different enzymatically-tagged competitive and sandwich immunoassay formats on a single chip platform. The insulin detection is based on a peroxidase (HRP)-labeled sandwich assay whereas the cortisol detection relies on an alkaline phosphatase (ALP)-labeled competitive immunoassay. The attractive analytical performance of the dual marker immunosensor, with no apparent cross-talk, was achieved through systematic optimization of the incubation and amperometric detection of the different captured enzyme tags. Evaluation of dual biosensor chip in untreated serum samples indicated favorable simultaneous detection of picomolar (pM) insulin and nanomolar (nM) cortisol concentrations in a single microliter sample droplet within less than 25min. The new dual immunosensor chip offers considerable promise for frequent decentralized testing of I and C towards a tighter glycemic control and improved management of diabetes.

1. Introduction

Major efforts have been made by the scientific community over the last decade for developing more advanced diabetes care and management towards a tighter glycemic control (Anderson et al., 2007). Current automated insulin delivery (AID) systems or artificial pancreas (AP) platforms are limited to single biomarker data input, involving interstitial glucose levels, and cannot fully account for the influence of other biomarkers affecting glycemic events through variety of factors, ranging from diet changes, exercise to exposure to stress (Dadlani et al., 2018). To account for such changes associated with the patient's daily routine, future AID systems should integrate additional inputs obtained with real-time or single-use sensing devices (Dias and Silva Cunha, 2018). Accordingly, there are urgent needs for point-of-care sensor devices that allow multiplexed detection of additional key diabetes biomarkers, and thus enabling fast, accurate and personalized treatment without the delay associated with centralized lab analyses. Recent efforts in this direction have led to the development of a dual-analyte glucose/insulin detection microchip based an integrated enzymatic/immunoassay approach (Vargas et al., 2019), and to a multiplexed microneedle-based sensing of ketone bodies along with glucose and lactate toward a timely management of diabetic ketosis/ketoacidosis (Teymourian et al., 2020).

Besides glucose, insulin is the most relevant biomarker for the management of type 1 diabetes (T1D) owing to its critical role in glucose metabolism towards maintaining normal blood glucose concentrations (Wilcox, 2005). The release of insulin into blood is stimulated by an increase in the level of circulating blood glucose. Cortisol is another important biomarker linked to elevated hyperglycemia (glucose > 180mg/dL) during high-stress periods and to the regulation of blood glucose levels (Hackett et al., 2016; Kamba et al., 2016; Sher, 2005). Based on the major impacts of cortisol on insulin secretion and on glucose metabolism, the development of a sensor chip for detecting cortisol and insulin in point-of-care settings would help guiding AP platforms and greatly benefit people with diabetes towards a tighter

* Corresponding author.
** Corresponding author.
E-mail addresses: dassau@seas.harvard.edu (E. Dassau), josephwang@eng.ucsd.edu (J. Wang).

https://doi.org/10.1016/j.bios.2020.112512
Received 28 May 2020; Received in revised form 4 August 2020; Accepted 11 August 2020
Available online 15 August 2020

glycemic control (Andrews et al., 2002; Baron et al., 1987; Chiodini et al., 2007; Couch, 1992; De Feo et al., 1989; Plat et al., 1996; Van Cauter et al., 1992). However, despite of the growing needs for such a multiplexed insulin-cortisol detection in diabetes control, achieving this goal remains elusive as current clinical set-ups rely on centralized laboratories which provide only a periodic snapshot of insulin and cortisol levels (following long delays) instead of a true representation of their dynamically-changing concentrations.

In this work, we present a dual electrochemical immunosensor microchip toward fast, on-the-spot simultaneous detection of insulin and cortisol in a single microliter sample droplet through a single-step immunoreaction on a single biochip. Such a dual C/I sensor was realized by integrating competitive and sandwich immunoassay formats on a single platform along with the use of different (ALP and HRP) enzyme tags (generating reaction products that do not interfere at the neighboring electrode) along with different detection potentials to eliminate cross-reactivity during such single-chip simultaneous immunoassays. As illustrated in Fig. 1, the dual C/I detection chip with the specific C and I antibody receptors, immobilized on the neighboring electrodes, was incubated for 20min with the human serum samples spiked with different C/I concentrations, along with the enzyme-tagged immunoreagents, to accomplish the simultaneous immunoreactions. This was followed by short (~1.5min) sequential amperometric transduction steps to eliminate the cross-talk between the enzyme substrates. The cortisol detection relies on a competitive immunoassay format using the ALP enzymatic tag along with 1-naphthyl phosphate (1-NPP) enzymatic substrate, while insulin detection is based on a HRP-tagged sandwich format bioassay employing 3,3′,5,5′-tetramethylbenzidine (TMB)/H_2O_2 as the mediator/substrate redox system. Such choice of the enzyme tags, along with the selection of the corresponding detection potentials, ensures that their reaction products will not interfere with the neighboring electrode transduction process. Dual enzyme tagging-based multiplexed immunoassays have been previously studied in electrochemical (Zhang et al., 2016) and mainly in optical approaches (Basu et al., 2007; Jiang et al., 2013; Zhao et al., 2017). Yet, an integrated electrochemical immunoassay device combining ALP and HRP-based detection has not been previously reported.

To achieve successful implementation of such simultaneous multiplexed C/I microchip detection involving dual enzyme-tagging protocol, careful attention has been paid to addressing related operational and detection challenges, including (i) combining different competitive- and sandwich-based immunoassay formats; (ii) eliminating possible cross-talks during the recognition and particularly the amperometric transduction steps; (iii) addressing the largely different physiological concentration ranges of insulin (pM) and cortisol (nM); (iv) adapting a reliable and reproducible modification protocol to fabricate a compact dual immunochip on adjacent WEs using ultrasmall reagent volumes; and (v) achieving such ultra-sensitive assays using short analysis times and microliter sample volumes. By carefully addressing these challenges and judiciously optimizing the different immunorecognition and transduction steps, the resulting dual biosensor microchip offers an attractive analytical performance toward the simultaneous detection of the insulin and cortisol biomarkers in untreated serum samples. Such new capability holds considerable promise for multiplexed biomarker detection,

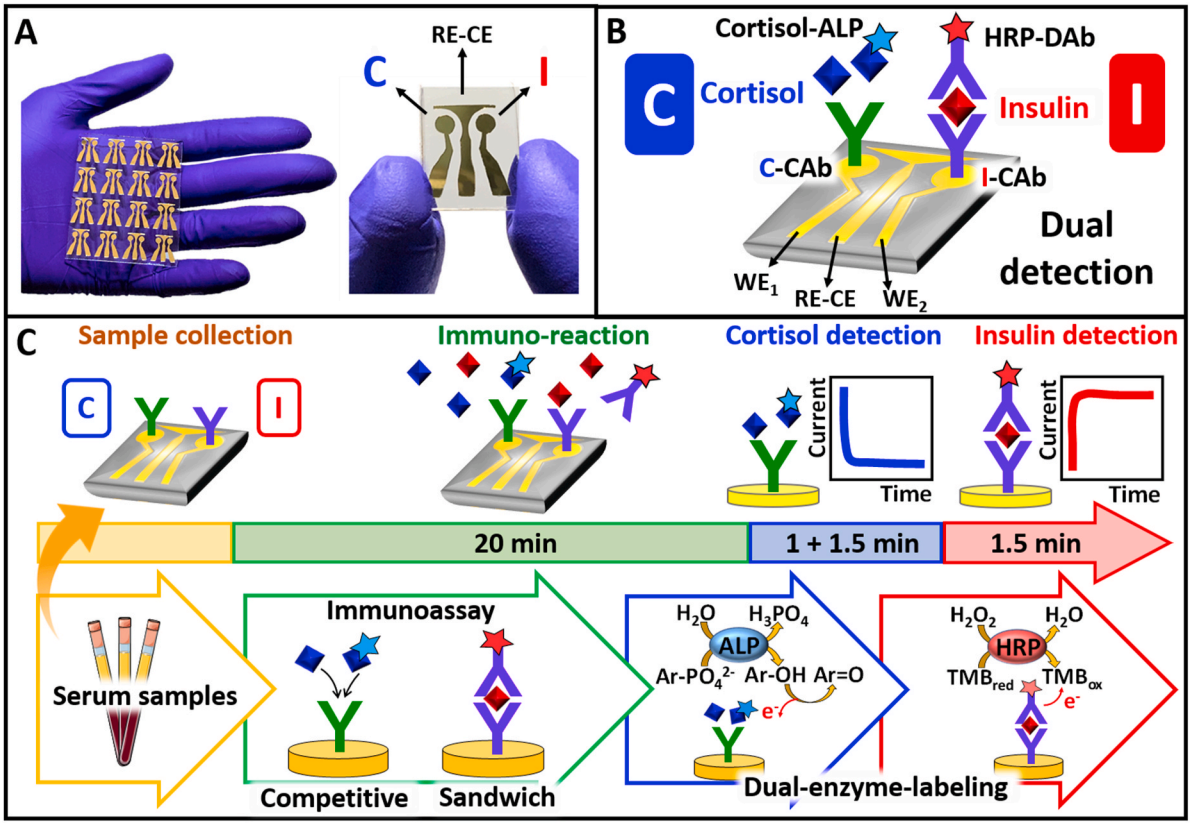

Fig. 1. The concept of dual C/I biosensor immunochip. A) Images of the Au sputtered 3-electrode system-based chip array on PETG substrate and a single sensor chip employed for dual C/I biosensor fabrication. B) Schematics of the ALP/HRP multi-enzymatic labeling based C/I dual sensor chip comprising two Au working electrodes (WE) modified with the bioreceptors for the C and I immunosensors, respectively, and a third Au electrode (in the middle) that acts as CE/RE. C) Immunoreaction and transduction processes involved in the C/I sensing. Cortisol and insulin detection are based on competitive and sandwich format immunoreactions, respectively, performed in a single simultaneous incubation step in which the sample is spiked with the HRP-DAb and C-ALP reagents. After 20min sample incubation, C detection is performed first through amperometric measurement at +0.4 V on Au WE1 through the oxidation of the phenolic product of the phosphate aromatic derivative hydrolysis catalyzed by the captured ALP tag. Finally, I is monitored on Au WE2 at -0.1 V by recording the cathodic current resulting of the activity of the HRP tag after washing the chip surface and adding the TMB/H_2O_2 redox substrate.

and particularly for diabetes management towards a tighter glycemic control.

2. Materials and methods

2.1. Equipment and instruments

A Barnstead Thermolyne (Type 16700 Mixer) vortex for homogenization of the solutions and pH/ISE meter (Orion Star A214 model) from Thermo-Scientific were used. All chronoamperometric responses were obtained using a μAutolab type III PGSTAT302N potentiostat (Metrohm) controlled by GPES software v 1.11.2. All the experiments were performed with homemade dual chip electrodes (Vargas et al., 2019), consisting of two Au-sputtered working electrodes (2.0mm diameter each) and a central joint Au counter-reference electrode.

2.2. Reagents, solutions and samples

All the reagents used in this work are of the highest purity grade. Commercial phosphate buffer solution (1.0 M), 11-mercaptoundecanoic acid (MUA), 6-mercapto-1-hexanol (MCH), 1-ethyl-3-(3-(dimethylamino)propyl) carbodiimide (EDC), N-hydroxysuccinimide (NHS), ethanolamine hydrochloride (≥%99), 2-(N-morpholino)ethanesulfonic acid (MES), 1-Naphthyl phosphate (1-NPP), 1-Naphthol (1-NPL) and sodium dodecyl sulfate (SDS) were acquired from Sigma-Aldrich. HPLC grade 2-propanol and sodium borate were obtained from Fisher Chemical, and pure ethanol from KOPTEC. 3,3′,5,5′-tetramethylbenzidine (TMB) substrate was purchased from Neogen (Enhanced K-Blue TMB Substrate, Neogen Life Sciences, USA). Tween-20 was obtained from Fisher Scientific. Cortisol capture antibody (C-CAb) and cortisol-3-alkaline phosphatase (C-ALP) were acquired from Fitzgerald Industries. Cortisol antigen (C) (hydrocortisone) was obtained from Sigma-Aldrich. Insulin capture antibody (I-CAb) and HRP-labeled insulin detection antibody (HRP-DAb) were purchased from US Biological and human insulin standard (I) from Sigma-Aldrich. Human serum samples were purchased from San Diego Blood Bank (SDBB).

The following buffer solutions, prepared with Milli-Q water, were used: phosphate buffer (PB) 0.1M, pH 7.4; phosphate buffer 0.1M, pH 7.4 containing 0.02% Tween-20 (PBT); MES 25mM, pH 6.5; borate buffer (BB) 5mM, pH 7.4 containing 5mM $MgCl_2$; borate buffer 5mM, pH 7.4 containing 5mM $MgCl_2$ and 0.02% Tween-20 (BBT). Stock solutions of 1μM Insulin and 10mg mL^{-1} cortisol were prepared in PB containing 32μM HCl and 0.02% Tween-20, and in ethanol, respectively.

2.3. Preparation of thin film Au sputtered electrodes

The electrode fabrication protocol was based on our previously reported procedure (Vargas et al., 2019), except that the final silver sputtering step was removed in the current procedure to simplify the fabrication approach. Therefore, Au was used for both working and reference/counter electrodes in this work without compromising the performance. Briefly, 0.76mm thick PETG (glycol-modified polyethylene terephthalate) sheets (Small Parts Inc.) were used as the substrate. Cricut machine was used to create the designed mask through cutting the laminated protective cover of the substrate. First, a Chromium (Cr) layer was sputter deposited onto the polymer substrate, acting as adhesion layer, using a Denton Discovery 18 Sputter System under direct current (DC) mode at 200 W for 20s, under Argon (Ar) gas pressure of 2.4mTorr. This was followed by gold (Au) sputtering in DC mode at 200 W for 5min, under Ar gas pressure of 2.4mTorr. Finally, two 10-min washing steps in isopropyl alcohol and water were performed to clean the electrodes.

2.4. Dual C/I chip modification and immunoassay protocols

The procedure applied for C/I chip preparation is summarized in Fig. S1 in the Supplementary Information and involves the following steps: after cleaning and drying the electrodes, they immersed in an alkanethiol mixture solution consisting of MUA (0.1mM) and MCH (1.0mM) and kept overnight at 4°C under humid conditions. The SAM-functionalized electrodes were washed by pure ethanol and water, 10min each. All the following steps were performed at room temperature under humid conditions by drop casting 2.5μL on the surface of each working electrode with the appropriate solution according to the specific immunoassay. After each incubation step, the electrodes were rinsed with PB (0.1M, pH 7.4) and dried with compressed air gun.

The terminal carboxylic groups on the SAM-functionalized electrode surface were activated by incubation in a mixture solution of EDC (0.4M) and NHS (0.1M) prepared in MES buffer (25mM, pH 6.5) for 35min. Then, the electrodes were incubated in the capture antibody solution 200μg mL^{-1} (30min) or 100μg mL^{-1} (45min) for C or I immunoassay, respectively, followed by a 30min blocking step of the remaining free activated carboxylic groups with ethanolamine solution 2.0M for C and 1.0M for I immunoassay, respectively. After this step, the immunosensor electrodes were stored at 4°C for subsequent use.

A 20min incubation step was adapted for performing the immunoassays. Depending on the type of detection (individual or simultaneous), the incubation was carried out by placing a 2.5-μL sample droplet on the corresponding WE (individual) or by covering the whole chip involving the two WEs with a 10-μL drop (simultaneous). In the individual assays, the WE was exposed to the sample mixture prepared in PBT or serum containing cortisol and C-ALP (1:10 diluted) for the C immunoassay, and insulin and HRP-DAb (1μg mL^{-1}) mixture for the I immunoassay. In the case of simultaneous I and C detection, the 10-μL incubation drop contained all the necessary reagents for both immunoassays.

After this final step, the electrodes were washed first with SDS solution (0.05% SDS prepared in PB 0.1M, pH 7.4), and subsequently with PB (0.1M, pH 7.4), followed by air gun drying. The chronoamperometric measurements were preformed sequentially, first the C sensor and then the I sensor, applying +0.4 V and -0.1 V for 90 s, respectively. The cortisol detection is based on ALP/1-NPP (5.0mM) system, requiring 1min hydrolysis step before applying potential, whereas insulin detection employs H_2O_2/HRP/TMB system.

3. Results and discussion

A schematic display of the working principle employed in the dual-enzyme-based amperometric immunosensor chip for simultaneous detection of cortisol and insulin biomarkers is shown in Fig. 1. A plastic sheet comprising Au-sputtered electrode arrays is shown in Fig. 1A, with each sensor chip consisting of two WEs for C and I biomarkers and a third electrode in the middle acting as reference/counter (RE/CE). Fig. 1B illustrates the heterogeneity of the immunoassay format and the localized detection of each biomarker on the corresponding antibody bioreceptor-functionalized electrode, along with the transduction principle relying on different enzyme labeling strategies used for simultaneous detection of both analytes. The cortisol immunosensor relies on a competition reaction of the target cortisol antigen and the ALP-tagged cortisol (C-ALP) for the relevant capture antibody sites on the electrode surface, followed by amperometric detection of the hydrolytic reaction product of 1-NPP enzymatic substrate. In the case of insulin, a sandwich immunoassay format is adapted using horseradish peroxidase (HRP) as enzymatic label and 3,3′,5,5′-tetramethylbenzidine (TMB)/H_2O_2 as the mediator/substrate detection system. Fig. 1C shows the schematics of the various steps involved in the dual C/I assay and the duration of each step. Such simultaneous assay (within less than 25min) starts with a 20min simultaneous incubation of the microliter sample C/I mixture, containing known concentrations of the enzyme-tagged immunoreagents, with the surface-functionalized C and I capture antibodies. During this step, the C-ALP and the cortisol are recognized by the immobilized anti-cortisol capture antibody (C-CAb) in a competitive assay, while the insulin antigen is sandwiched by the HRP-labeled

detector anti-insulin antibody (HRP-DAb) and the immobilized anti-insulin capture antibody (I-CAb). The simultaneous incubation step is followed by sequential amperometric transduction reactions for C and I sensors. The ALP-based amperometric cortisol detection involves the biocatalytic hydrolysis of 1-NPP for 1min and monitoring the oxidation current of the enzymatic product 1-naphthol (1-NPL) at +0.4 V. This anodic current is directly proportional to the level of the captured ALP-tag and therefore it is inversely proportional to the cortisol concentration in the sample. The HRP-based insulin sensing relies on amperometric transduction through the HRP/H_2O_2/TMB redox probe, in which the cathodic current due to the HRP-catalyzed H_2O_2 reduction, mediated by TMB, is measured at -0.1 V (Kadir and Tothill, 2010; Kumar Ahirwal and Mitra, 2010). As expected for such sandwich immunoassay, the current response depends on the amount of the captured HRP tag which is proportional to the insulin concentration.

3.1. Cross-talk evaluation and performance optimization of the dual C/I enzyme immunoassay

In order to attain ultrasensitive sensing capability with the dual microchip, the experimental variables (during immunoreactions and electrochemical transductions) that affect the analytical performance were thoroughly examined and optimized. ALP is a hydrolase enzyme able to catalyze the hydrolysis of nearly all phosphate monoesters into the inorganic phosphate ion and the corresponding alcohol, phenols, or saccharides (Sharma et al., 2014). ALP has been widely used as a tracer in immunosensors due to its suitability to electrochemical detection by generating a readily detected electroactive product from a non-interfering electroinactive substrate (Kreuzer et al., 1999). This enzyme exhibits highest catalytic activity and stability under alkaline conditions. As ALP has a broad substrate specificity, various compounds have been reported as enzyme substrates (Kreuzer et al., 1999; Pemberton et al., 1999; Preechaworapun et al., 2008). Of these, 1-NPP has been chosen in our protocol as it offers several advantages including electroinactivity over the conventional potential range, low oxidation potential of its enzymatic hydrolysis product, along with high sensitivity and stability. Fig. 2A shows the reaction sequence involved in transducing the present C immunoassay. 1-NPP is hydrolyzed upon reacting with ALP, giving rise to the electroactive product 1-NPL which subsequently undergoes oxidation to 1,4-naphthoquinone (1,4-NPQ) on the electrode surface. Similarly, in the case of I sensor, the current corresponds to the electrocatalytic response of the TMB/H_2O_2 couple, that serves as cosubstrate to HRP enzyme tag. The electrocatalytic reaction involved in the insulin detection, shown in Fig. 2B, involves the HRP biocatalytic reduction of H_2O_2 with the concurrent oxidation of TMB oxidation to TMB^+ continued by reduction of TMB^+ back to TMB on the electrode surface.

Buffers possessing a Tris-HCl type molecular structure would be preferred for ALP catalysis as they promote transphosphorylation of the substrates (Kreuzer et al., 1999). However, the optimum buffer should lead to low background currents along with a wide potential window and should support the product stability without any cross-reactivity with the reactants or products during the assay. Based on this, the electrochemical properties of different buffers on the sensor microchip system were explored by examining their catalytic activity and possible interference for 1-NPL oxidation monitoring (Fig. S2). Fig. S2A compares the current intensities measured by cyclic voltammetry (CV) on bare Au electrodes for Tris-HCl buffer and BB at alkaline pH 9.5. These experiments revealed the superior properties of BB as the preferred medium for performing the assay, as Tris-HCl displayed a large catalytic current on bare Au electrodes. Additionally, the amperometric behavior of these buffers was assessed with the C sensor in the absence and presence of incubation with C-ALP through monitoring of the current of 1-NPP substrate reaction at +0.4 V (see Fig. S2B). In agreement with the CV results, a lower background current and hence a wider current window was obtained in the BB solution (compared to Tris-HCl), suggesting the suitability of this buffer solution toward sensitive detection of cortisol.

The electrochemical behaviors of 1-NPP and its hydrolysis product, 1-NPL, were examined in BB solution by running CV at the bare Au electrode (Fig. 2C). As expected, 1-NPP was not electrochemically active over the potential range studied but 1-NPL displayed an irreversible chemical reaction due to its oxidation to the insoluble quinoid product (Preechaworapun et al., 2008). Moreover, CV measurements performed with the C sensor in absence and presence of C-ALP confirmed the specificity of the transduction reaction involving the oxidation of the enzymatically generated naphthol derivative in the presence of ALP (Fig. 2E). Similarly, the CV of the commercial TMB/H_2O_2 was carried out on the bare Au electrode (Fig. 2D), revealing solely the characteristic H_2O_2 reduction peak obtained at negative currents, since in the absence of HRP the TMB oxidation by H_2O_2 is a remarkably slow process (Zhou et al., 2016). As illustrated in the CVs recorded with the I sensor, once the HRP-tagged sandwich immunocomplex is formed (Fig. 2F), the reversible TMB oxidation reaction takes place in the HRP-catalyzed H_2O_2 detection, resulting in low-potential redox peaks and more importantly, without additional peaks at potentials close to +0.4 V which is essential to obviate any cross-talks during the simultaneous C/I assays. Based on the obtained results, amperometric measurements under applied potentials of +0.4 V and -0.1 V were chosen for signal transduction of the C and I immunosensors, respectively. To demonstrate the selectivity of these operating potentials toward simultaneous dual analyte measurements, amperometric currents obtained for each analyte were compared at these potentials. Fig. 2G displays a well-defined discrimination on the C sensor for blank vs C-ALP-incubated electrodes at +0.4 V; however, no response is observed for C measurements performed at -0.1 V. Similarly, for the I sensor (Fig. 2H), while a distinct response is observed using a potential of -0.1 V, measurements performed at +0.4 V (used for the C detection) did not exhibit any response to 1nM insulin. Overall, the above observations suggest the suitability of using different applied potentials (along with the different enzyme tags) for selective amperometric detection of 1-NPL product (at +0.4 V) and H_2O_2 substrate (at -0.1 V) for detecting C and I, respectively, in an integrated dual microchip without apparent cross reactivity.

The development of the highly sensitive immunosensing systems requires the optimization of various important parameters affecting the performance of the dual enzymatic reactions, including buffer properties, reaction time and substrates concentration. For cortisol amperometric immunoassay, the effect of parameters affecting the ALP activity was evaluated (Fig. S3), including the concentration and hydrolysis time of 1-NPP substrate, and concentration of $MgCl_2$ as the presence of Mg^{2+} ions has shown to enhance the biocatalytic hydrolysis reaction rate (Rej, 1977). As expected, the longer hydrolysis time generated a larger amount of 1-NPL and thus, a higher amperometric signal (Fig. S3A). Nevertheless, it was realized that after carefully optimizing other variables including 1-NPP and $MgCl_2$ concentrations along with the C-ALP concentration (Fig. S3B), it was possible to adopt 1min hydrolysis time as it could provide sufficient signal to noise ratio to enable sensitive cortisol immunoassays. Indeed, the slightly lower amperometric signal obtained with 1min, compared to 10min hydrolysis time, is compensated by the significantly shorter reaction time. After optimizing the transduction conditions for C sensor, the parameters involved in immunorecognition were systematically optimized toward a fast (20min) and sensitive assay (Fig. S4A). The optimum values for concentration and incubation time of C-CAb were found to be 200μg mL^{-1} and 30min, whereas the 1:10 dilution of commercially supplied C-ALP corresponding to $10U_{ALP}$ mL^{-1} was obtained as its optimum concentration. In case of the I sensor, the experimental and transduction conditions were similar to those used earlier (Vargas et al., 2019). However, in order to adapt a simultaneous dual analyte measurement which can be performed in 20min, the immunoreaction recognition steps of both analytes were merged into a single step and the concentration of HRP-labeled insulin antibody was optimized (Fig. S4B), resulting in an

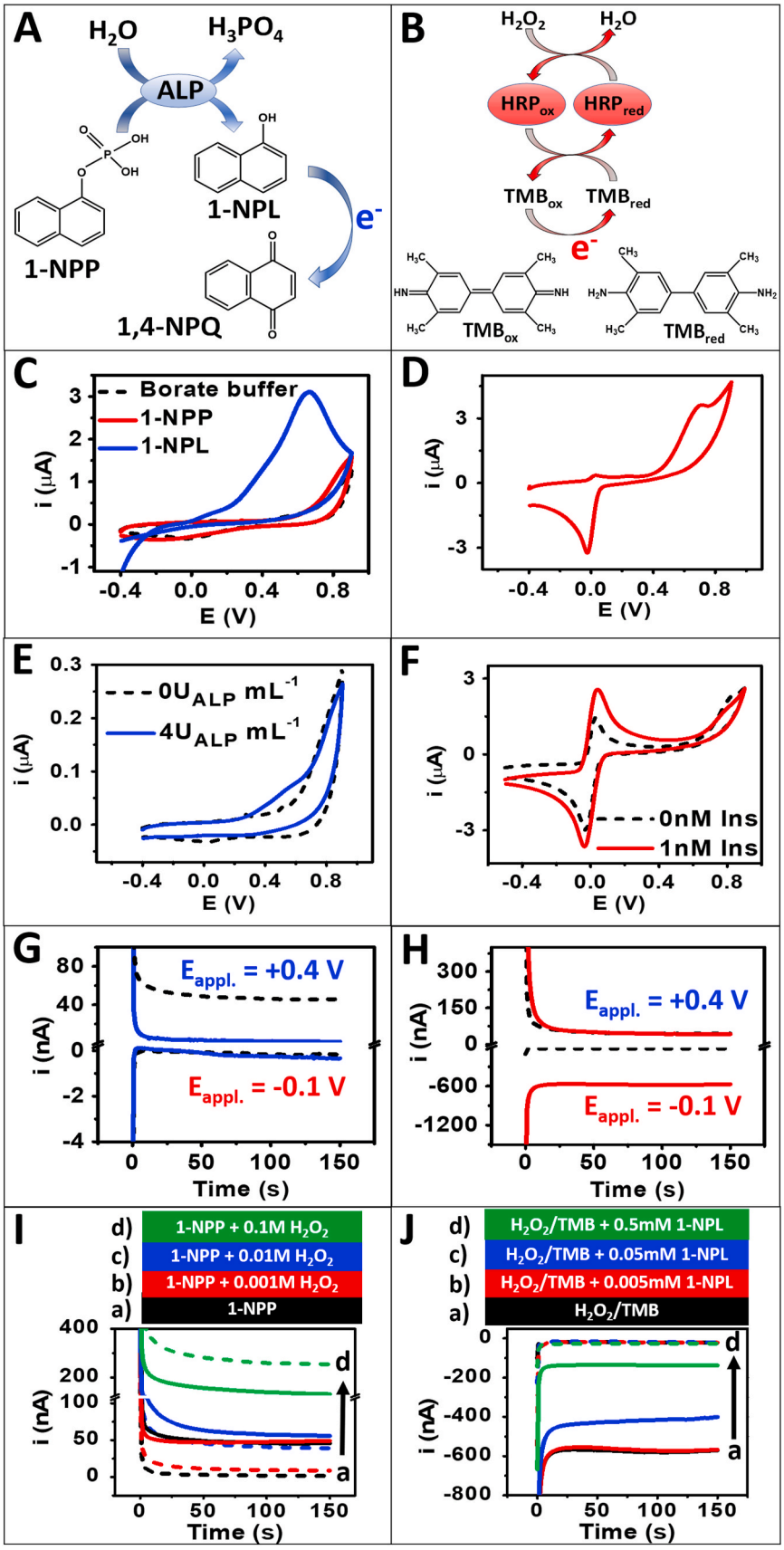

Fig. 2. Cross-talk evaluation during electrochemical transduction for C/I dual analyte microchip electrodes. A,B) The schematic representation of ALP- (A) and HRP-mediated (B) enzymatic reactions. C). The CVs of 1-NPP and 1-NPL (5 mM) in BB solution (5mM, pH 9.5) containing 5mM Mg^{2+} ions on the bare Au microelectrode. D) CV of the commercial TMB/H_2O_2 on the bare Au microelectrode. E) CVs recorded for 1-NPP (5mM) on the C immunosensor in absence and presence of C-ALP conjugate. F) CVs of insulin immunosensor incubated in 0 and 1nM insulin concentration and 1μg mL^{-1} of HRP-DAb conjugate. Operating potentials for cortisol and insulin detection were +0.4 V and -0.1 V, respectively. G) Amperometric response of the C sensor incubated with 0 (dashed curve) and 100ng mL^{-1} cortisol (blue curve) recorded under different potentials of +0.4 V and -0.1 V. C-ALP was 10 times diluted. H) Amperometric response of the I sensor incubated with 0 (dashed curve) and 1nM insulin (red curve) and recorded at different applied potentials of +0.4 V and -0.1 V. The concentration of HRP-DAb was 1μg mL^{-1}. I) Amperometric response of the C microchip to 0 (dashed curves) and 100ng mL^{-1} cortisol (solid curves) obtained in different mediator solutions of 5mM 1-NPP (black) and 1-NPP containing varying levels of H_2O_2. J) Amperometric response of the I microchip to 0 (dashed curves) and 1nM insulin (solid curves) obtained in different mediator solutions of TMB/H_2O_2 (black) and TMB/H_2O_2 containing varying levels of 1-NPP. (For interpretation of the references to colour in this figure legend, the reader is referred to the Web version of this article.)

optimal value of 1μg mL^{-1}.

Considering that each sensor could present different optimal buffer pH for the biorecognition and transduction reactions, we carried out a comprehensive study to attain the most appropriate conditions that accommodate these immunoassay schemes towards simultaneous C/I detection with the dual sensor microchip. As illustrated in Fig. S5A, which shows the effect of pH on the ALP-based hydrolysis reaction rate, the highest amperometric response is observed when the ALP-catalyzed 1-NPP hydrolysis occurs in BB at pH 9.5; in contrast (and as expected), the minimal enzymatic activity is observed when the hydrolysis reaction was performed in PB solution at pH 7.4 as the PB can lead to saturate the active sites of the ALP enzyme (Zhang et al., 2004). On the other hand, the evaluation of the pH effect on the sample incubation step for C (Fig. S5B) and I (Fig. S5C) immunosensors indicated that the most favorable performance of both sensors is observed at pH value of 7.4. The similar optimum pH for the incubation step on both immunosensors clearly indicates the possibility of combining the immunorecognition steps for the C/I dual sensor chip into a single incubation step, towards a greatly simplified multiplexed immunoassay protocol.

Upon establishing the optimal C/I immunoreaction protocol, it was important to assess the cross-talk between the two neighboring C and I sensors during the transduction procedures for the dual captured enzyme tags towards possible simultaneous amperometric readout of the two target analytes. Toward this, the possible effect of H_2O_2 on the ALP-based transduction was first examined (Fig. 2I) through measuring the current signals obtained for electrodes incubated with the blank and C-ALP conjugate (1:10 diluted) solutions in the presence of varying concentrations of H_2O_2. As can be seen, false positive amperometric responses were obtained in the presence of H_2O_2, which can be ascribed to the catalytic oxidation of 1-NPL by H_2O_2 (Cheneviere et al., 2010; Yan et al., 2000). In the same way, the insulin detection performance was assessed in the presence of varying concentrations of 1-NPL (Fig. 2J). As shown, 1-NPL negatively affected the current signal of the I sandwich-based immunoassay, which may be ascribed to the catalysis effect of peroxidase on the oxidation of 1-NPL and the accumulation of the generated insoluble oxidation product, 1,4-naphthoquinone, on the electrode surface that may passivate the electrode (Liang et al., 2013; Preechaworapun et al., 2008). Based on these results, a sequential readout protocol was adapted for the enzymatic reactions. The order in which the sequential electrochemical transduction should be carried out and the physical disposition of the corresponding enzyme substrate solution were evaluated (Fig. S6). It can be concluded from the results that the ALP-based 1-NPP hydrolysis reaction on the cortisol electrode should be performed first, followed by a washing step and the HRP-based H_2O_2/TMB electrode reaction. The order of performing the transduction reactions is important as the opposite order (I first followed by C) resulted in inferior performance, which is attributed to the adsorption and passivation of the RE/CE Au electrode surface by the oxidized mediator, TMB_{ox}, and thus compromising the successive ALP-based transduction (Baldrich et al., 2009; Luo et al., 2020).

3.2. Analytical performance of the dual C/I sensor chip

The electrochemical sensing performance and operational characteristics of the dual biosensor chip were evaluated toward rapid and sensitive simultaneous detection of C and I biomarkers. The analytical performance of each immunoassay was first characterized individually by detecting increasing concentrations of the C and I analytes in PBT using an ultrasmall sample volume of 2.5μL. The resulting amperometric signals and the corresponding calibration plots are shown in Fig. 3A. A linear dependence between the amperometric response and the cortisol concentration is observed for the C sensor over the range from 0 to 250ng mL^{-1}, with the maximum signal corresponding to 0ng mL^{-1} C. On the other hand, the sandwich-based I immunoassay resulted in a well-defined response to the 200pM I increments and a linear correlation between the current response and the I concentration ranging from 0 to 1000pM. The limits of detection (LOD), estimated from the calibration data, were 13.4ng mL^{-1} and 30.6pM for C and I, respectively. These results clearly demonstrate the suitability of the dual immunosensor to detect these biomarkers at their physiological levels, as required in clinical analysis.

The potential cross-reactivity between the dual target analytes during sample incubation step was carefully examined for each sensor by measuring the response of each sensor in the presence of a mixture containing a fixed concentration of one analyte along with varying levels of the second one. As demonstrated in Fig. 3B, the cortisol and insulin signals are not affected by increasing levels of insulin and cortisol, respectively, indicating no apparent cross-talk effect. These data thus support the specificity of this dual analyte assay and hence the feasibility of the optimized one-step analysis protocol toward the simultaneous detection of these biomarkers.

In order to demonstrate the applicability of the fabricated C/I chips for the simultaneous detection of cortisol and insulin, the dual-analyte microchips were incubated for 20min with 10 μL sample droplets of PBT solutions containing HRP-DAb and C-ALP, along with increasing concentrations of both biomarkers (in 50ng mL^{-1} and 200pM steps for C and I, respectively). A sequential electrochemical detection protocol is thus performed in which the C transduction is first carried out, involving 1min of 1-NPP substrate hydrolysis and 1.5min of signal measurement. This C detection is followed by a washing step and the use of the H_2O_2/TMB redox probe for 1.5min for the I detection. As shown in Fig. 3C, distinct signal increments are observed upon increasing target biomarker concentrations in all cases. Such well-defined amperometric responses of dual-analyte immunosensor toward simultaneously detecting increasing levels of C and I along with the resulted calibration plots demonstrated the minimal cross-talk and reliability of the developed multiplexed analytical protocol. Additionally, the sensitivities achieved for both biomarkers using this simultaneous single-chip measurements (Fig. 3C) were similar to those obtained for individually detecting immunosensor chips (Fig. 3A), indicating that the sensitivities are not affected by simultaneous incubation of the reagents. Obviously, having a single I/C chip, along with a single immunoreaction step, greatly simplifies the requirements of point-of-care testing. For the fabricated microchips to be reliably applied toward point-of-care decentralized testing, the different sensors should provide highly reproducible results for a fixed analyte concentration. The amperometric signals from six different dual C/I chips, shown in Fig. 3D, toward a PBT solution containing 50ng mL^{-1} cortisol and 1000pM insulin yielded RSD values of 3.4% and 4.9% for C and I detection, respectively. In addition, the dual biosensor chip was exposed to C–I mixture solutions with different varying concentrations ranging between 50 and 500ng mL^{-1} and 250–1000pM for cortisol and insulin analytes, respectively. The amperometric responses obtained for cortisol (blue curves) and insulin (red curves), represented in Fig. 3E, highlight the proven capability of the novel dual biosensor to perform simultaneous C/I detection with negligible cross-talk between neighboring sensor platforms.

3.3. Applicability of the dual C/I chip in serum cortisol and insulin detection

Serum is a very valuable biological specimen in monitoring patients as it does not contain blood cells and clotting factors which can interfere with the analysis, but its composition possesses proteins and other biomolecules of interest and thus, representing a comprehensive view of the body. The applicability of the dual biosensor chip was explored towards decentralized on-the-spot analysis of cortisol and insulin by performing direct detection of these biomarkers in untreated serum samples, which were acquired from San Diego Blood Bank. The analytical performance of the C/I sensors in such a matrix was first evaluated individually by incubating each biosensing platform with a 2.5μL serum sample spiked with the corresponding enzymatic tracer and increasing concentrations of the target biomarkers, ranging from 0 to 400ng mL^{-1} for cortisol and

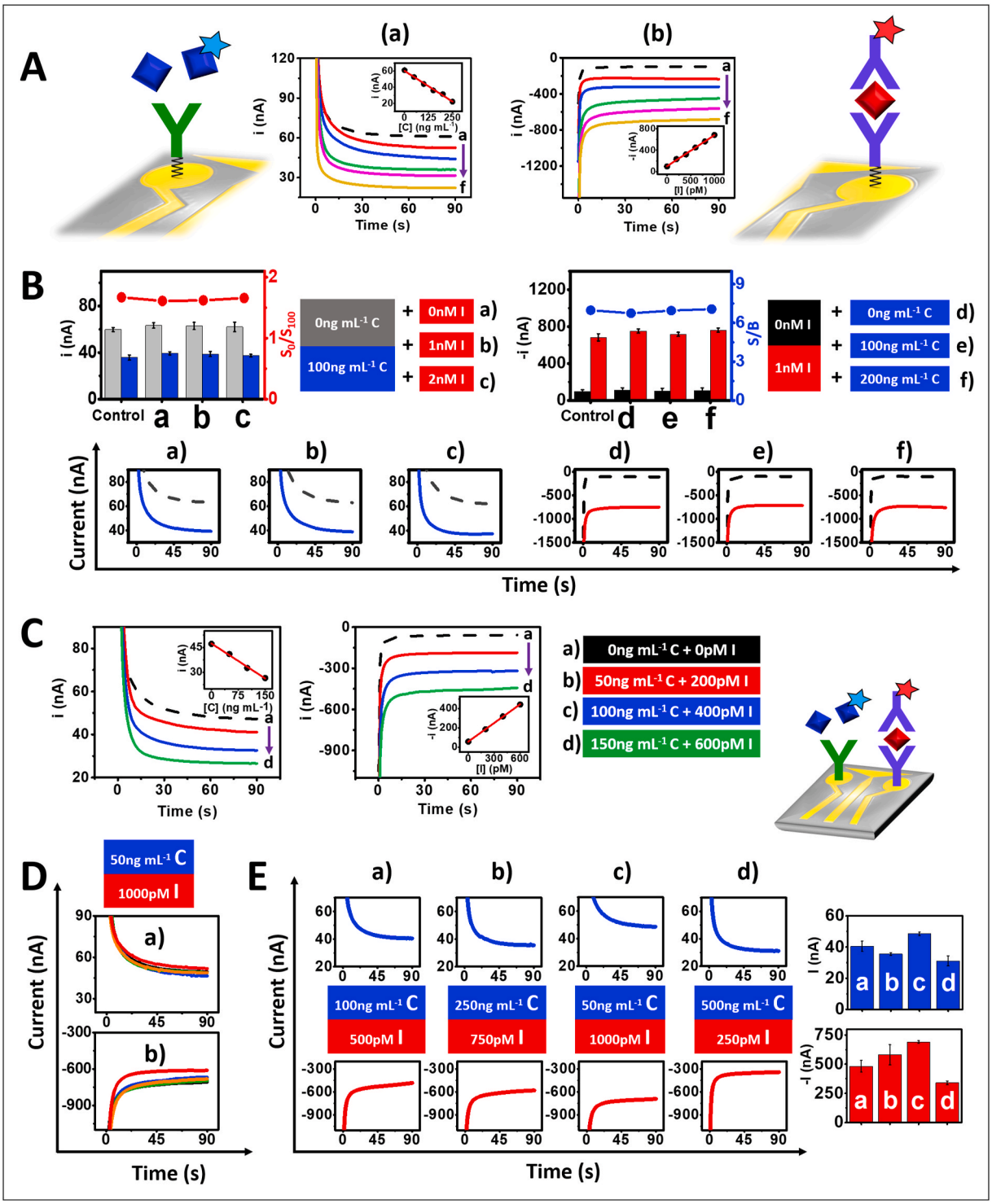

Fig. 3. Electrochemical sensing performance of C/I dual chips in PB solution. A) Amperometric response of C (a) and I (b) sensors to increasing concentrations of cortisol from a) 0 to f) 250ng mL^{-1} with 50ng mL^{-1} increments, and insulin from a) 0 to f) 1000pM with 200pM increments, respectively. Insets are the corresponding calibration plots. B) Immuno-reaction related cross-talk evaluation towards cortisol and insulin simultaneous detection: amperometric signals recorded with C sensor for 0 (grey dashed curves) and 100ng mL^{-1} cortisol (blue curves) in absence (control) and presence of 1μg mL^{-1} of HRP-DAb and a) 0nM, b) 1nM and c) 2nM insulin; amperometric signals recorded with I sensor for 0 (black dashed curves) and 1nM insulin (red curves) in absence (control) and presence of 1:10 diluted C-ALP and a) 0ng mL^{-1}, b) 100ng mL^{-1}, c) 200ng mL^{-1} cortisol. Error bars represent the standard deviation of the measurements performed with three different chips. C) Amperometric response obtained in the simultaneous detection of increasing C/I concentrations in a single microliter (10μL) sample droplet containing both biomarkers from (a) 0ng mL^{-1} cortisol + 0pM insulin (black curves) to (d) 150ng mL^{-1} cortisol + 600pM insulin (green curves), with increments of 50ng mL^{-1} and 200pM for cortisol and insulin, respectively. Insets are the corresponding calibration plots. D) Reproducibility of 6 dual sensor chips in the measurement of a mixture containing a) 50ng mL^{-1} cortisol and b) 1nM insulin. E) Amperometric response for simultaneous detection of different cortisol/insulin mixtures whose concentrations range from 50 to 500ng mL^{-1} for cortisol (blue curves) and from 250 to 1000pM for insulin (red curves). Error bars represents the standard deviation of the measurements performed with three different chips. (For interpretation of the references to colour in this figure legend, the reader is referred to the Web version of this article.)

0–4nM for insulin (Fig. 4A). In both cases, well-defined amperometric curves were obtained with currents corresponding to the changes in the levels of the cortisol and insulin biomarkers, although the values of the amperometric responses were lower than those obtained in the buffer matrix, indicating some degree of biofouling occurred on the electrode surface. However, both sensors demonstrated attractive performance towards simultaneous detection of both serum analytes in a minimum volume of sample droplet, with LOD values of 23.1ng mL^{-1} and 177pM for cortisol and insulin, respectively, thus covering clinically relevant concentration ranges of these biomarkers. In order to assess the viability of simultaneous dual marker detection, the C/I biosensor chips were exposed to 10μL-drop of untreated serum spiked with increasing concentrations of both analytes, ranging from 0 to 300ng mL^{-1} for cortisol and from 0 to 3nM for insulin. As can be observed from the amperometric curves shown in Fig. 4B, the dual analyte sensor chip responded conveniently to 100ng mL^{-1} and 1nM concentration increments for cortisol and insulin, respectively, in a time frame shorter than 25min. Furthermore, in agreement with the data of Fig. 3, very similar sensitivities were obtained for these serum matrices using the individual (Fig. 4A) and simultaneous (4 B) detection procedures, further supporting the diagnostic utility of our developed immunoassay chip for point-of-care dual analyte sensing. Finally, the reproducibility assessment of simultaneous dual analyte measurements in a serum sample containing 100ng mL^{-1} cortisol and 1nM insulin yielded RSD values of 5.1% for C and 7.1% for I (n = 5), which further demonstrates the robustness and reliability of the optimized fabrication and analytical protocols for the new dual-biomarker biosensor device (Fig. 4C).

4. Conclusions

This work reports on the first example of a disposable dual electrochemical sensor microchip for simultaneous, on-the-spot detection of cortisol and insulin toward advanced diabetes management. The developed dual sensing chip relied on coupling, on a single disposable platform and within a single incubation step, the competitive and sandwich immunoassay formats with fundamentally distinct ALP and HRP enzymatic tagging strategies. Achieving such an attractive analytical performance in the ultrasensitive simultaneous amperometric C and I detection, using significantly different analyte concentration levels, without cross talk of the neighboring sensors, required critical attention to key challenges of performing such bioassay using a single sample microdroplet. Sensitive and direct simultaneous detection of cortisol and insulin in untreated microliter blood serum samples was realized within 25min. Overall, the developed C/I sensor chip represents a promising

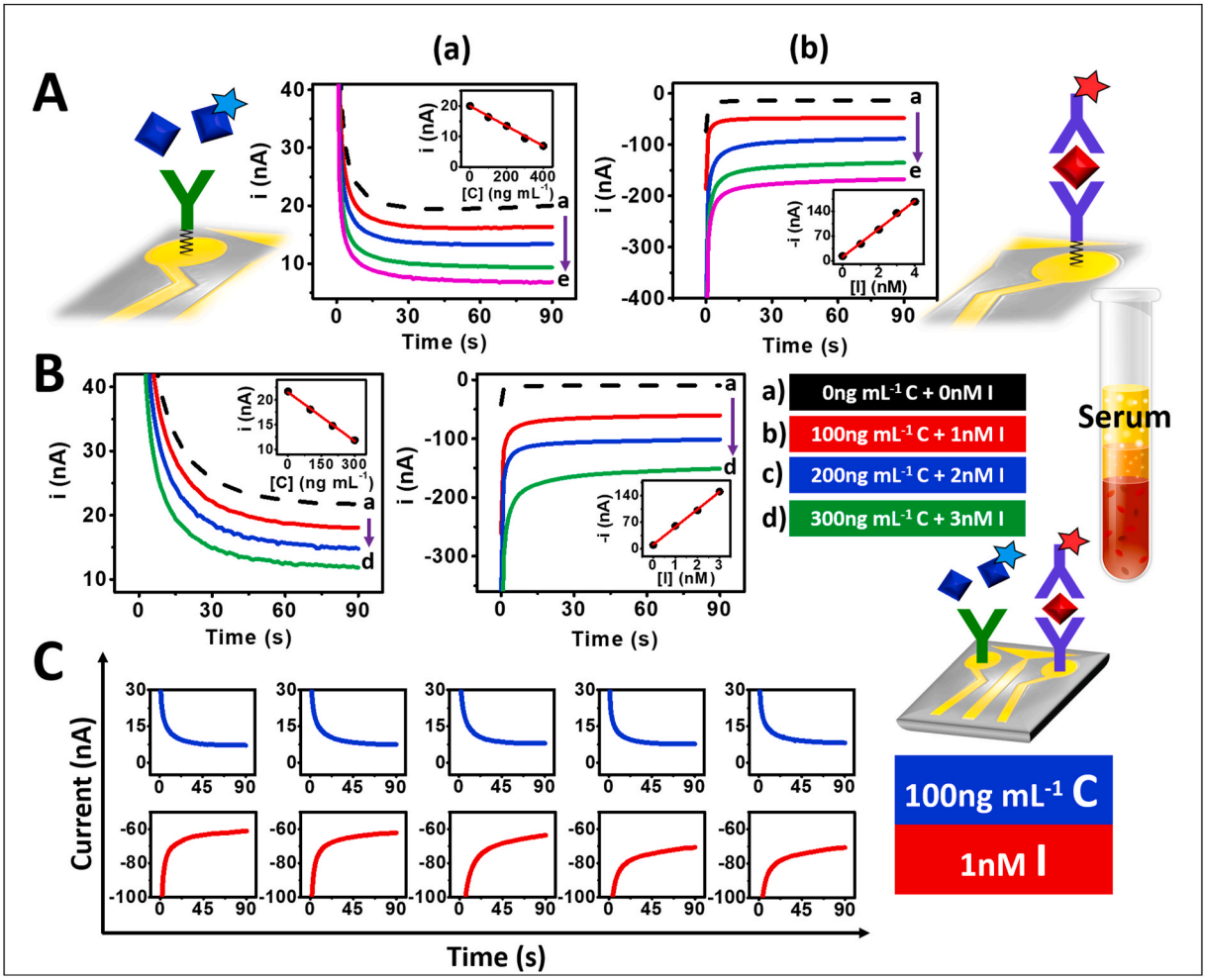

Fig. 4. Electrochemical sensing performance of C/I dual chips in non-treated human serum. A) Amperometric response of C (a) and I (b) sensors to increasing concentrations of cortisol from a) 0 to e) 400ng mL^{-1} with 100ng mL^{-1} increments, and insulin from a) 0 to e) 4nM with 1nM increments, respectively. Insets are the corresponding calibration plots. B) Amperometric response obtained in the simultaneous detection of increasing concentrations of C/I in a single serum sample droplet containing increasing levels of biomarkers from (a) 0ng mL^{-1} cortisol + 0pM insulin (black curves) to (d) 300ng mL^{-1} cortisol + 3nM insulin (green curves), with increments of 100ng mL^{-1} and 1nM for cortisol and insulin, respectively. Insets are the corresponding calibration plots. C) Reproducibility of the dual sensor chip in the measurement of a mixture containing cortisol 100ng mL^{-1} (blue curves) and insulin 1nM (red curves). (For interpretation of the references to colour in this figure legend, the reader is referred to the Web version of this article.)

technology for rapid decentralized screening and testing of these important diabetes biomarkers towards guiding the automated insulin delivery, enhancing glycemic control, and improving the management of diabetes. The concept can be adapted to microfluidics-based, automated dual biosensing assay, and can be expanded further towards the frequent monitoring of additional biomarkers that affect glycemic events. The new immunoassay format opens also attractive opportunities towards multienzyme tagged bioassays for multiplexed detection of biomarkers panels. Future efforts are being focused on the extensive validation of the developed dual marker chip in diabetic patients, against currently available centralized laboratory immunoassay protocols, to meet the requirements of point-of-care clinical settings.

CRediT authorship contribution statement

Eva Vargas: Methodology, Formal analysis, Investigation, Visualization, Writing - original draft, Writing - review & editing, Experimental design. **Eloy Povedano:** Formal analysis, Investigation, Visualization, Writing - original draft. **Sadagopan Krishnan:** Experimental design, Methodology, Formal analysis, Investigation, and, Visualization. **Hazhir Teymourian:** Writing - original draft, Writing - review & editing, Experimental design. **Farshad Tehrani:** Fabrication. **Susana Campuzano:** Experimental design, Writing - review & editing. **Eyal Dassau:** Experimental design, Funding acquisition, Project administration, Supervision, Writing - review & editing. **Joseph Wang:** Resources, Funding acquisition, Project administration, Visualization, Supervision, Writing - review & editing, Experimental design.

Declaration of competing interest

The authors declare that they have no known competing financial interests or personal relationships that could have appeared to influence the work reported in this paper.

Acknowledgments

This work is supported by The Leona M. and Harry B. Helmsley Charitable Trust (Grant number 2018PG-TI0061). E.P. acknowledges support from the Spanish Ministerio de Economia y Competitividad (BES-2016-076606). S.K. is grateful to Prof. Joseph Wang for sponsoring his sabbatical year at UCSD during 2019–2020.

Appendix A. Supplementary data

Supplementary data to this article can be found online at https://doi.org/10.1016/j.bios.2020.112512.

References

Anderson, J.L., Carlquist, J.F., Roberts, W.L., Horne, B.D., May, H.T., Schwarz, E.L., Pasquali, M., Nielson, R., Kushnir, M.M., Rockwood, A.L., Bair, T.L., Muhlestein, J. B., 2007. Am. Heart J. 153, 1.
Andrews, R.C., Herlihy, O., Livingstone, D.E.W., Andrew, R., Walker, B.R., 2002. J. Clin. Endocrinol. Metab. 87 (12), 5587, 559.
Baldrich, E., del Campo Francesc, F.J., Muñoz, F.X., 2009. Biosens. Bioelectron. 25, 920–926.
Baron, A.D., Wallace, P., Brechtel, G., 1987. Diabetes 36, 1230–1237.
Basu, A., Maitra, S.K., Shrivastav, T.G., 2007. Anal. Biochem. 366, 175–181.
Cheneviere, Y., Caps, V., Tuel, A., 2010. Appl. Catal., A 387, 129–134.
Chiodini, I., Adda, G., Scillitani, A., Coletti, F., Morelli, V., Di Lembo, S., Epaminonda, P., Masserini, B., Beck-Peccozi, P., Orsi, E., Ambrosi, B., Arosio, M., 2007. Diabetes Care 30, 83–88.
Couch, R.M., 1992. Acta Endosc. 127, 115–117.
Dadlani, V., Pinsker, J.E., Dassau, E., Kudva, Y., 2018. Curr. Diabetes Rep. 18, 88.
De Feo, P., Perriello, G., Torlone, E., Ventura, M.M., Fanelli, C., Santeusanio, F., Brunetti, P., Gerich, J.E., Boll, G.B., 1989. Am. J. Physiol. 257 (1 Pt 1), E35–E42.
Dias, D., Silva Cunha, J.P., 2018. Sensors-Basel 18 (8), 2414. https://doi.org/10.3390/s18082414.
Hackett, R.A., Kivimäki, M., Kumari, M., Steptoe, A., 2016. J. Clin. Endocrinol. Metab. 101 (2), 619–625.
Jiang, W., Wang, Z., Beier, R.C., Jiang, H., Wu, Y., Shen, J., 2013. Anal. Chem. 85, 1995–1999.
Kadir, M.K.A., Tothill, E., 2010. Toxins 2, 382–398.
Kamba, A., Daimon, M., Murakami, H., Otaka, H., Matsuki, K., Sato, E., Shinobu, T., Takayasu, S., Matsuhasi, Y., Yanagimachi, M., Terui, K., Kageyama, K., Tokuda, I., Takahashi, I., Nakaji, S., 2016. PloS One 11 (11) e0166077.
Kreuzer, M.P., O'Sullivan, C.K., Guibault, G.G., 1999. Anal. Chim. Acta 393, 95–102.
Kumar Ahirwal, G., Mitra, C.K., 2010. Biosens. Bioelectron. 25, 2016–2020.
Liang, G., Liu, X., Li, X., 2013. Biosens. Bioelectron. 45, 46–51.
Luo, M., Xue, X., Rao, H., Wang, H., Liu, X., Zhou, X., Xue, Z., Lu, X., 2020. Sensor. Actuator. B Chem. 309, 127707.
Pemberton, R.M., Hart, J.P., Stoddard, P., Foulkes, J.A., 1999. Biosens. Bioelectron. 14, 495–503.
Plat, L., Byrne, M.M., Sturis, J., Polonsky, K.S., Mochezl, J., Fery, F., Van Cauter, E., 1996. Am. J. Physiol. 270 (1 Pt 1), E36–E42.
Preechaworapun, A., Dai, Z., Xiang, Y., Chailapakul, O., Wang, J., 2008. Talanta 76, 424–431.
Rej, R., 1977. Clin. Chem. 23, 1903–1911.
Sharma, U., Pal, D., Prasad, R., 2014. Indian J. Clin. Biochem. 29, 269–278.
Sher, L., 2005. Q. J. Med. 98, 323–329.
Teymourian, H., Moonla, C., Tehrani, F., Vargas, E., Aghavali, R., Barfidokht, A., Tangkuaram, T., Mercier, P.P., Dassau, E., Wang, J., 2020. Anal. Chem. 92, 2291–2300.
Van Cauter, E., Shapiro, E.T., Tillil, H., Polonsky, K.S., 1992. Am. J. Physiol. 262 (4 Pt 1), E467–E475.
Vargas, E., Teymourian, H., Tehrani, F., Eksin, E., Sánchez-Tirado, E., Warren, P., Erdem, A., Dassau, E., Wang, J., 2019. Angew. Chem. Int. Ed. 58, 6376–6379.
Wilcox, G., 2005. Clin. Biochem. Rev. 26 (2), 19–39.
Yan, Y., Xiao, F.S., Zheng, G., Zhen, K., Fang, C., 2000. Mol. Catal. A-Chem. 157, 65–72.
Zhang, L., Buchet, R., Azzar, G., 2004. Biophys. J. 86 (6), 3873–3881.
Zhang, N., Ma, Z.Y., Ruan, Y.F., Zhao, W.W., Xu, J.J., Chen, H.Y., 2016. Anal. Chem. 88 (4), 1990–1994.
Zhao, L., Wang, D., Shi, G., Lin, L., 2017. J. Lumin. 32, 1547–1553.
Zhou, X., Jiang, Y., Zaijun, L., Zhiguo, G., Guangli, W., 2016. Spectrochim. Acta Mol. Biomol. Spectrosc. 165, 106–113.